Classical Initial Conditions for Nucleus-Nucleus Collisions

Yuri Kovchegov

Department of Physics

University of Washington

Seattle, WA

USA

Heavy Ion Collisions

It is believed that the partons (quarks and gluons) liberated in a heavy ion collision through interaction form a thermally and (possibly) chemically equilibrated gas of quarks and gluon – quark-gluon plasma.

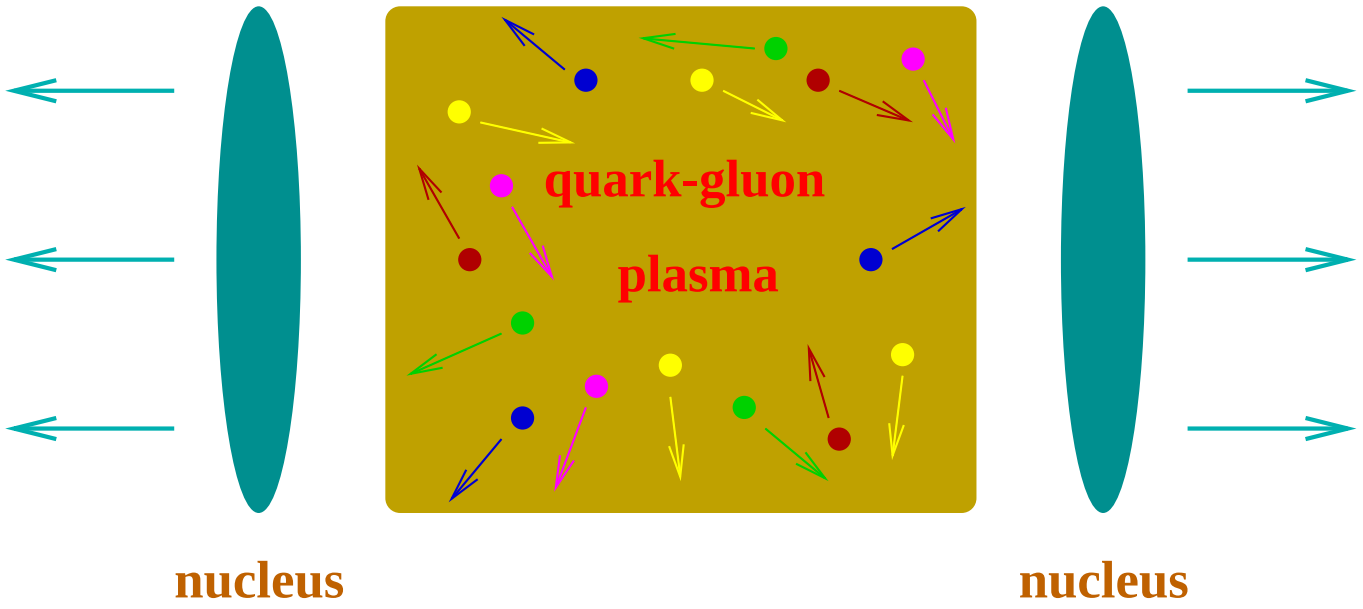

Figure 1: Formation of Quark–Gluon Plasma (QGP) in a Heavy Ion Collision.

One needs to consistently understand using QCD at least in some simplified limit whether this is what really happens in heavy ion collisions and if yes then how exactly in happens.

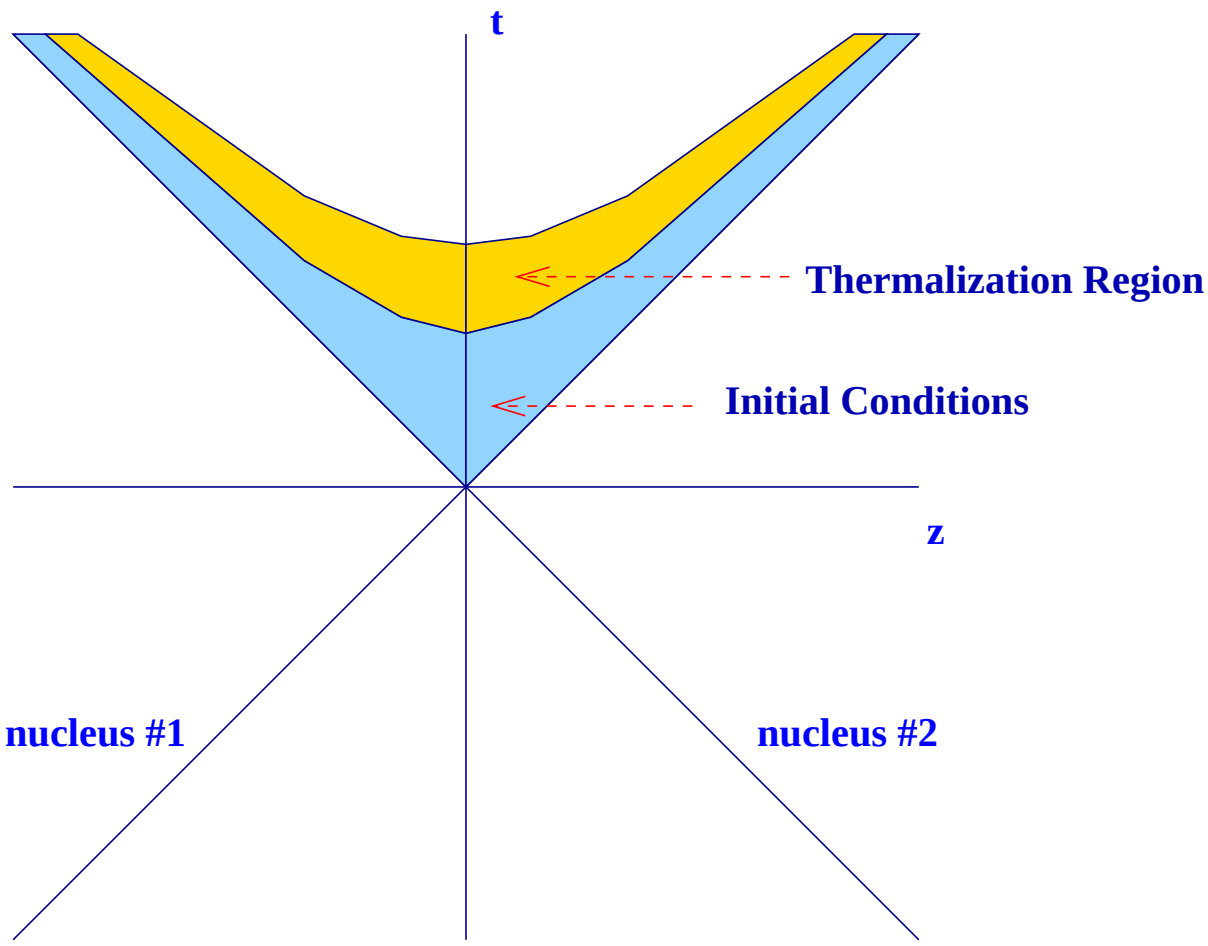

Figure 2: Space-time picture of a Heavy Ion Collision.

First few stages following a heavy ion collision:

1. Creation of gluons and quarks - construction of initial conditions.

2. Possible thermalization of quarks and gluons.

Our goal here is to determine the distribution of gluons in the state immediately following the collision — the initial conditions for QGP formation.

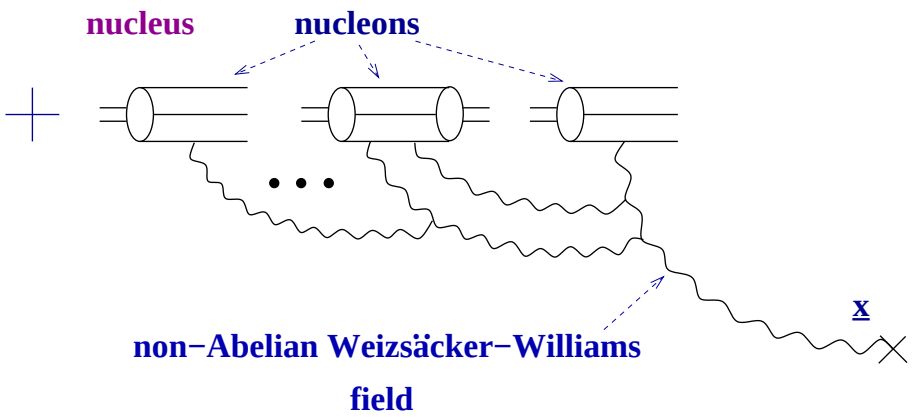

Figure 3: Non-Abelian Weizsäcker-Williams field of a large nucleus.

$$\underline{A}^{WW}(\underline{x}, x_-) \;=\; \int\; d^2z\; dz_-\theta(z_- - x_-)\; \hat{\rho}^a(\underline{z}, z_-)\; \frac{\underline{x}-\underline{z}}{|\underline{x}-\underline{z}|^2}$$

$$\times S_0(\underline{x}, z_-) T^a S_0^{-1}(\underline{x}, z_-)$$

with the gauge rotation matrix given by a path-ordered integral

$$S_0(\underline{x}, x_-) = \mathrm{P} e^{igT^a \int\; d^2z\; dz_-\theta(z_- - x_-)\; \hat{\rho}^a(\underline{z}, z_-)\; \ln(|\underline{x}-\underline{z}|\mu)}.$$

$\hat{\rho}^a$ is a color charge density operator normalized according to

$$\left\langle \hat{\rho}^a(\underline{x}, x_-)\; \hat{\rho}^b(\underline{y}, y_-) \right\rangle \;=\; \frac{\alpha_S}{2N_c\pi}\, \rho(\underline{x}, x_-)\, \delta(x_- - y_-)\, \delta^2(\underline{x}-\underline{y})\, \delta^{ab}$$

with $\rho(\underline{x}, x_-)$ the normal nuclear density in the infinite momentum frame of the nucleus, obeying

$$\int\; d^2x\; dx_-\; \rho(\underline{x}, x_-) = \; A.$$

This field represents the wave function of a large nucleus. One can look at the distribution of partons in this wave function.

$$k\,\frac{dN}{dk^2} \propto \langle\, A_\mu\, A_\mu \,\rangle$$

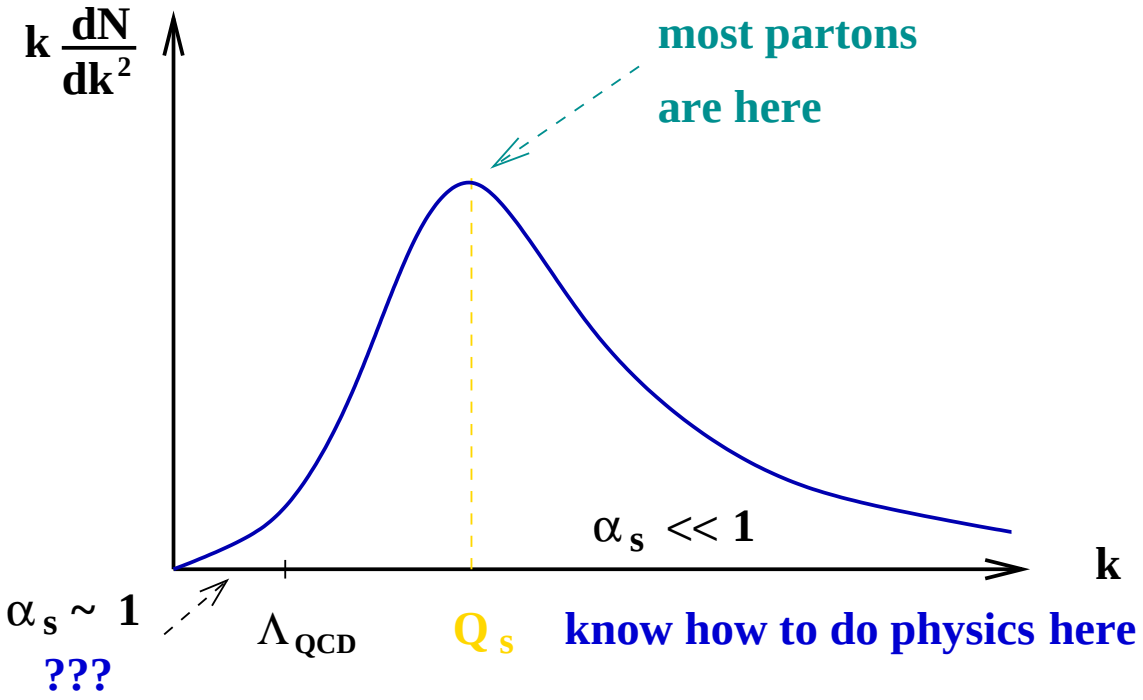

Figure 4: Distribution of partons in the nuclear wave function.

Most partons in the nucleus are distributed around the saturation momentum

$$Q_s^2 \sim A^{1/3} \Rightarrow Q_s^2 \gg \Lambda_{QCD}^2$$

which can get big for a large nucleus (heavy ion).

Expansion parameter:

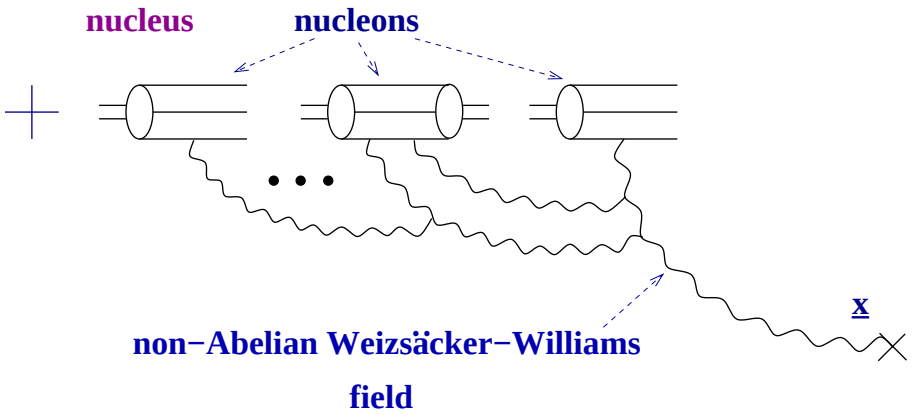

Figure 5: Classical field of a large nucleus.

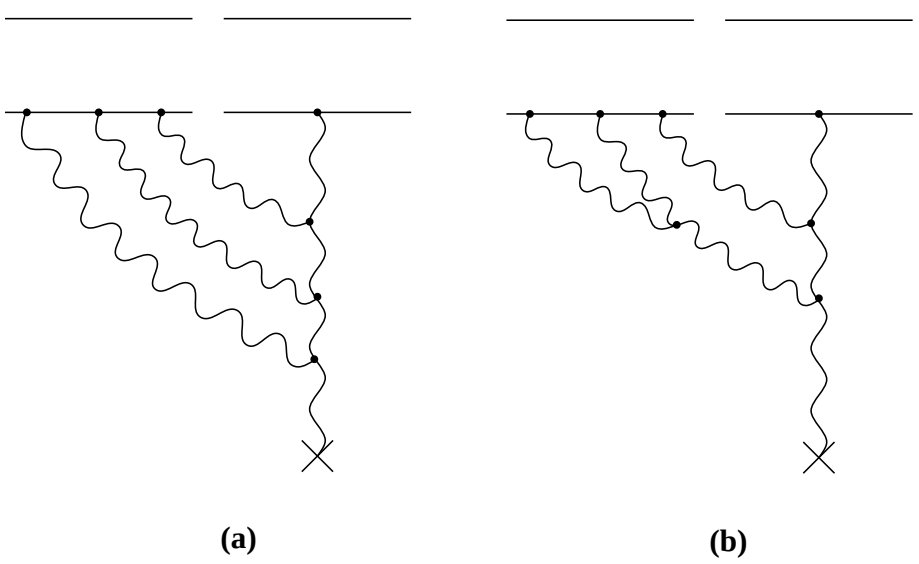

Figure 6: (a) A typical "classical" diagram at the order g^7, (b) a "quantum correction" diagram which is not included in the classical field at order g^7, but doesn't vanish.

$\Rightarrow$ Classical field dominates as long as there is no more than two gluons per nucleon in the diagrams!

Yu. K. '97

To include multiple rescatterings in the nuclear collisions one needs to find the classical field of two ultrarelativistic nuclei.

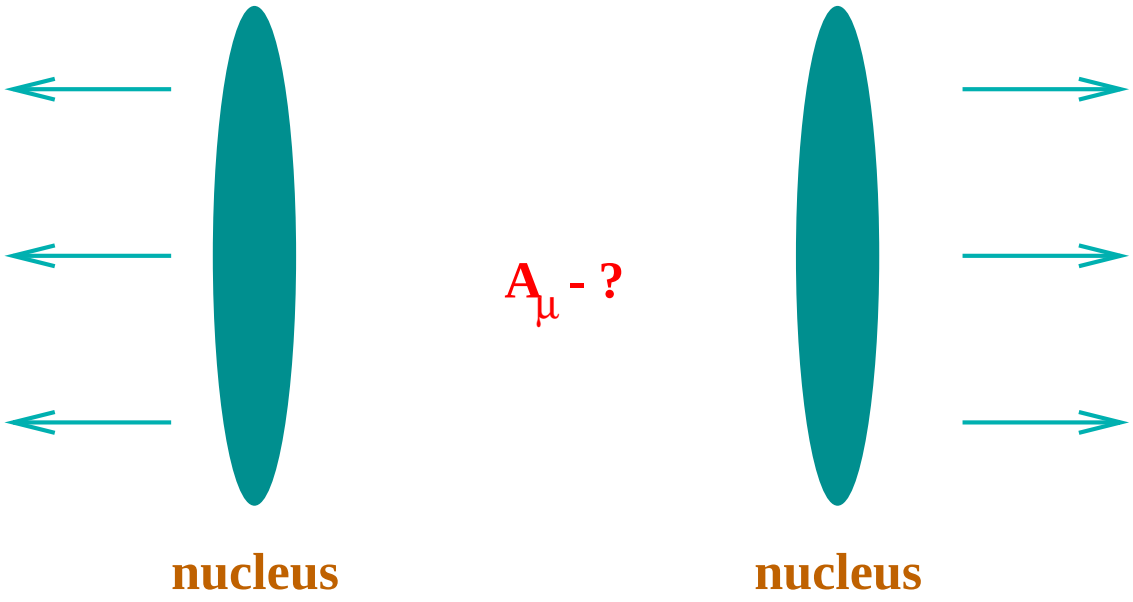

Figure 7: Classical field of two nuclei.

The complete classical field has not been found. However, there have been several attempts to find a perturbative part of the solution:

A. Kovner, L. McLerran, H. Weigert, '95; Yu. K. , D. Rischke, '97; S. Matinian, B. Muller, D. Rischke, '97; A. Krasnitz, R. Venugopalan, '98-'99; S. Bass, W. Poschl, B. Muller, '98-'99.

In a high energy nuclear collision the partons sitting in the nuclear wave function are instantaneously set free. Thus the distribution of the produced partons should be closely related to the distribution of the partons inside the nuclei before the collision.

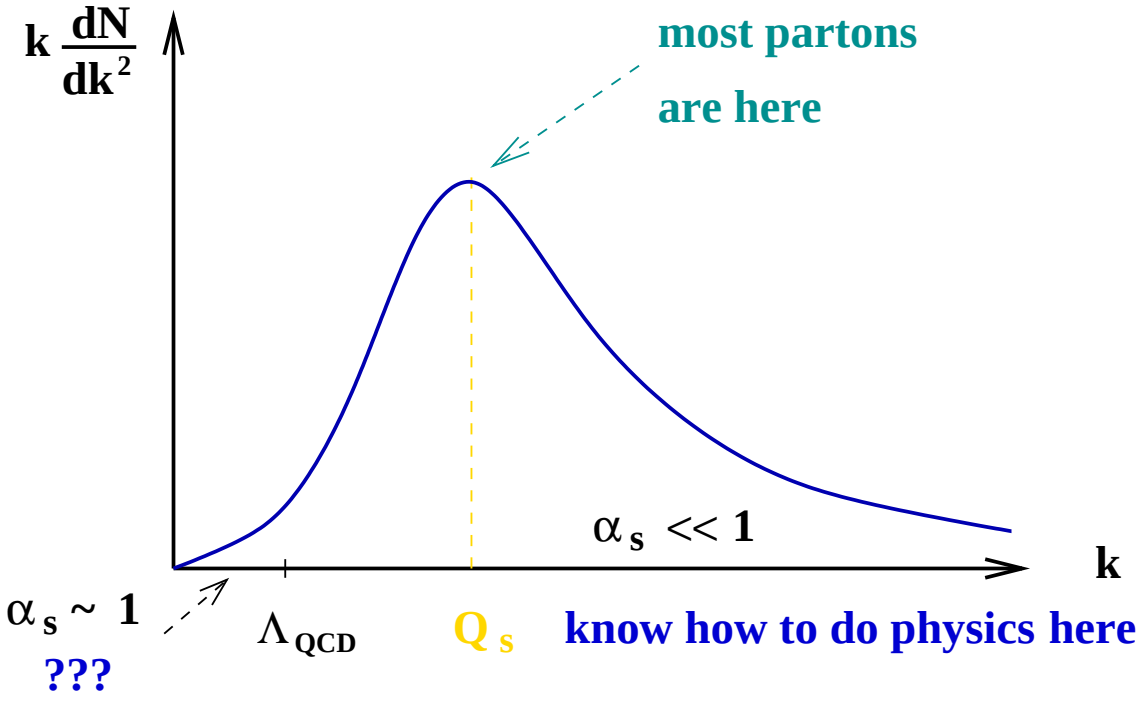

Figure 8: Distribution of partons in the nuclear wave function.

Thus one can conjecture that the typical momentum of the produced particles will be $k \sim Q_s \gg \Lambda_{QCD}$ and the evolution of the system could be described by weak coupling physics as $\alpha_s(Q_s) \ll 1$!!!

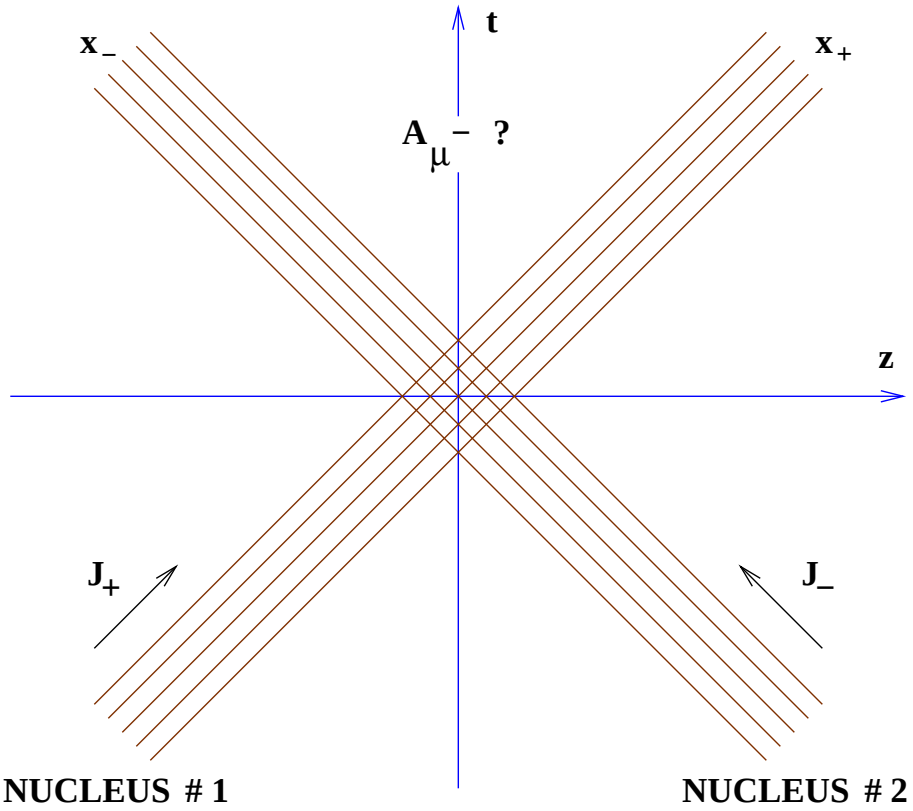

Figure 9: A collision of two ultrarelativistic nuclei at high energies.

Lowest order in α_s:

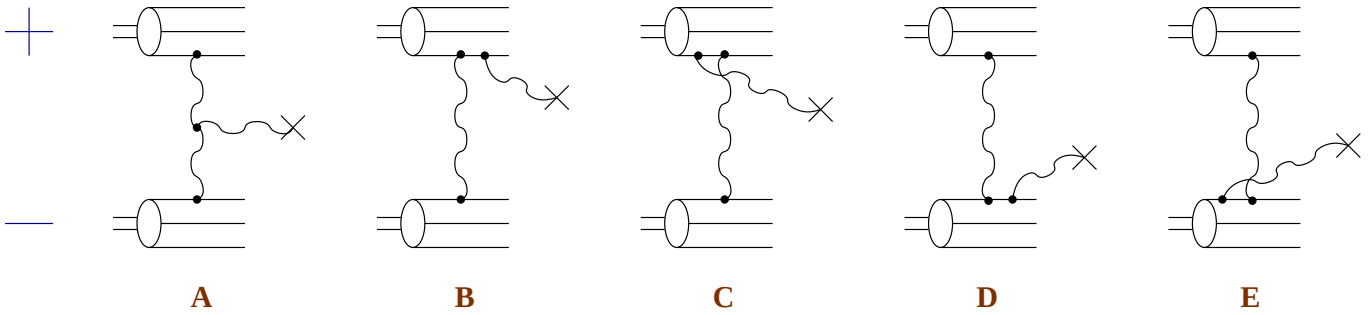

Figure 10: Diagrams contributing to the classical gluon field in covariant gauge at order g^3.

A. Kovner, L. McLerran, H. Weigert '95;
Yu. K., D. Rischke, '97;
M. Gyulassy, L. McLerran '97

Proton–Nucleus Collisions (pA)

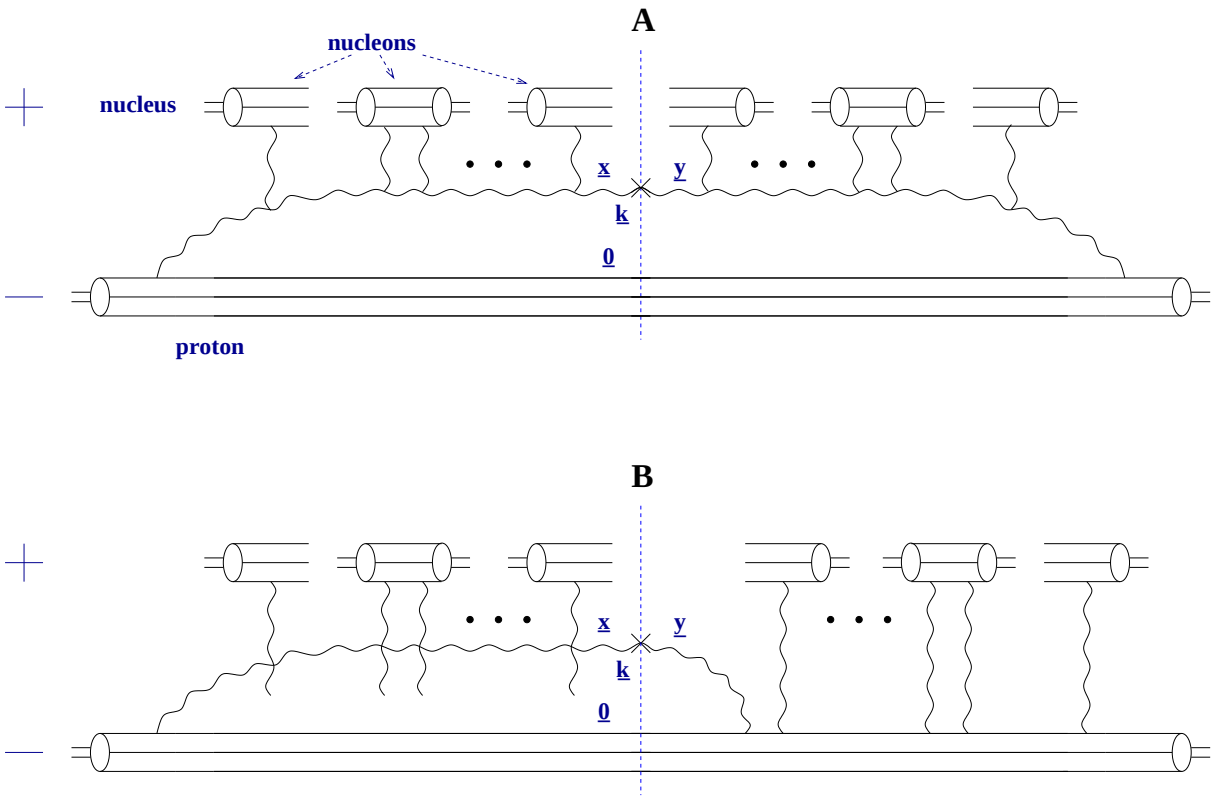

Figure 11: Covariant gauge (or more accurately $A_- = 0$ gauge) gluon production diagrams for proton–nucleus collision. Multiple rescatterings in the nucleus determine the interactions in this gauge.

$$\frac{d\sigma_1^{pA}}{d^2k\ dy} = \frac{1}{\pi}\int d^2b\, d^2x\, d^2y\, \frac{1}{(2\pi)^2}\,\frac{\alpha_S C_F}{\pi}\,\frac{\underline{x}\cdot\underline{y}}{\underline{x}^2\underline{y}^2}\, e^{i\underline{k}\cdot(\underline{x}-\underline{y})} \times\left(e^{-(\underline{x}-\underline{y})^2\ Q_s^2/4}-1\right)$$

$$\frac{d\sigma_{2+3}^{pA}}{d^2k\ dy} = \frac{1}{\pi}\int d^2b\, d^2x\, d^2y\, \frac{1}{(2\pi)^2}\,\frac{\alpha_S C_F}{\pi}\,\frac{\underline{x}\cdot\underline{y}}{\underline{x}^2\underline{y}^2}\, e^{i\underline{k}\cdot(\underline{x}-\underline{y})} \times\left(1-e^{-\underline{x}^2\ Q_s^2/4}+1-e^{-\underline{y}^2\ Q_s^2/4}\right).$$

Yu. K., A. H. Mueller, '98

Same pA process in $A_+ = 0$ light cone gauge

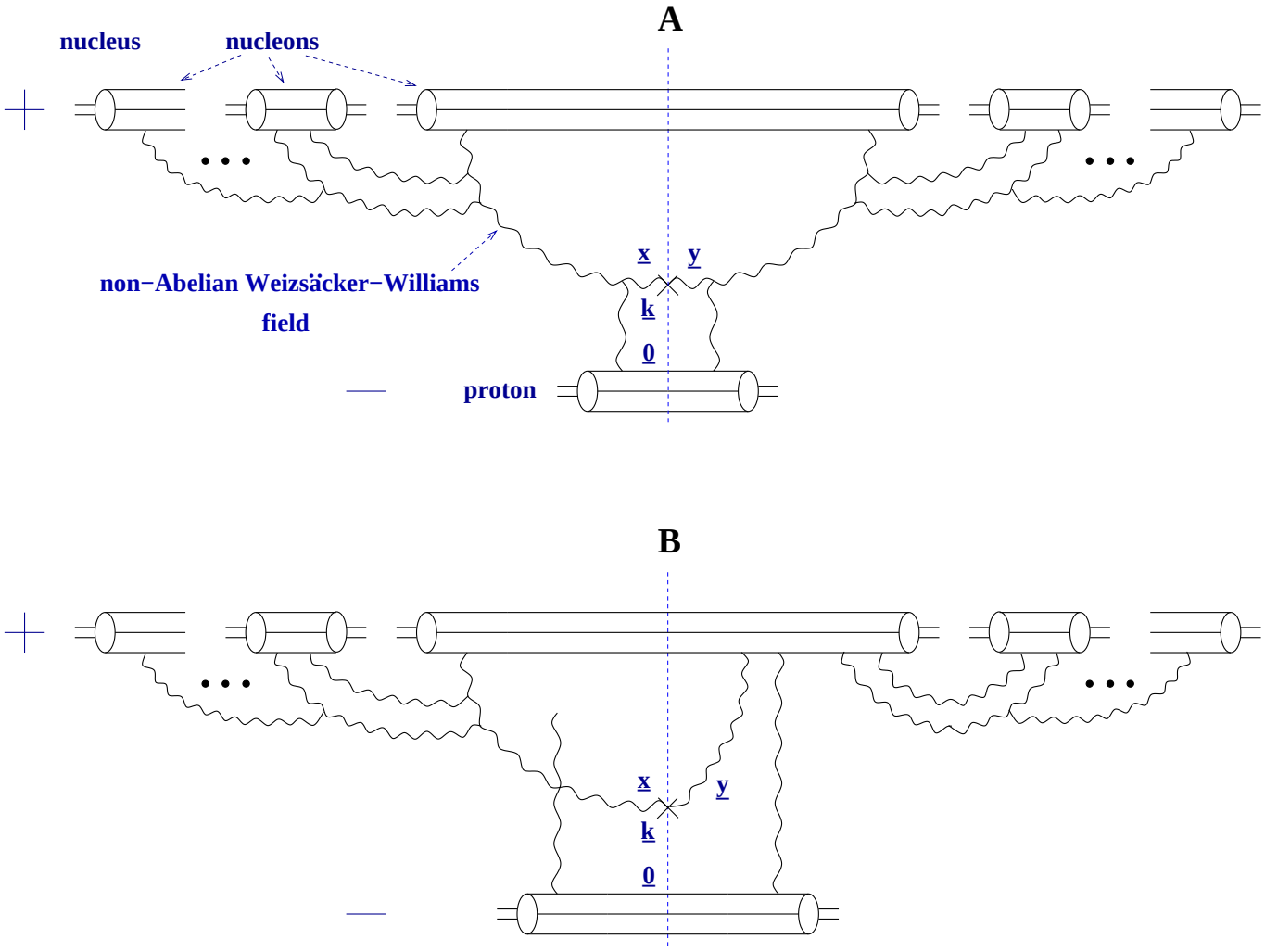

Figure 12: Gluon production in proton–nucleus collisions in $A_+ = 0$ light cone gauge.

Yu. K., hep-ph/0011252

Let us adopt a different strategy: we know the answer. Let us guess which diagrams give the same answer in $A_+ = 0$ light cone gauge. The diagrams are shown above.

The first diagram gives:

$$\frac{d\sigma^{pA}_{LC1}}{d^2k\ dy} = \int \frac{d^2x\ d^2y}{(2\pi)^2}\, e^{i\underline{k}\cdot(\underline{x}-\underline{y})}\, \frac{2}{\pi}\, \mathrm{Tr}\, \left\langle \underline{A}^{WW}(\underline{x}) \cdot \underline{A}^{WW}(\underline{y}) \right\rangle$$

$$\times \frac{-\alpha_S \pi^2 N_c}{N_c^2 - 1}\, (\underline{x}-\underline{y})^2\, xG(x, 1/(\underline{x}-\underline{y})^2).$$

where as we remember

$$\mathrm{Tr}\, \left\langle \underline{A}^{WW}(\underline{x}) \cdot \underline{A}^{WW}(\underline{y}) \right\rangle = \frac{C_F}{\pi \alpha_S (\underline{x}-\underline{y})^2} \left(1 - e^{-(\underline{x}-\underline{y})^2 Q_s^2/4} \right).$$

$\Rightarrow$ After the dust settles we observse that the diagram is equal to the symmetric diagram in covariant gauge.

$\Rightarrow$ A similar calculation shows the equivalence of the second diagram to the interference term in covariant gauge.

$\Longrightarrow$ We conclude from this analysis that the final state interactions cancel in $A_+ = 0$ light cone gauge in proton–nucleus collisions!!!

The following diagrams with final state interactions cancel for gluoproduction in pA:

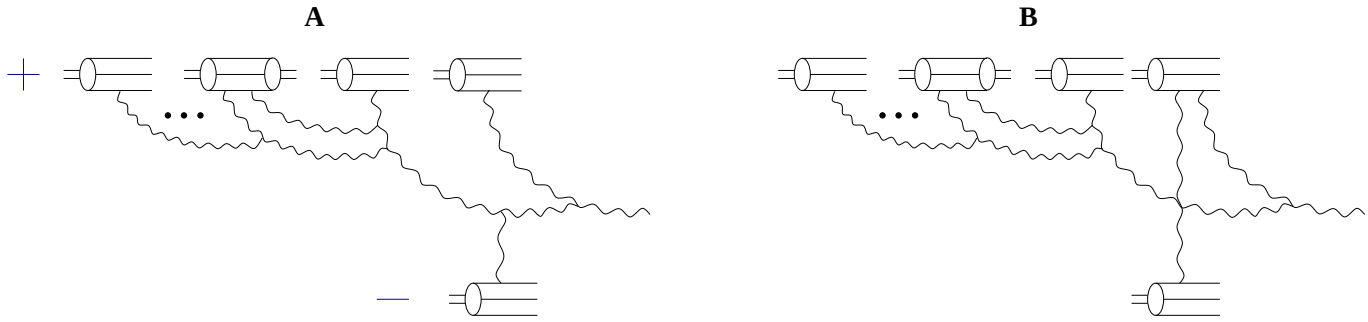

Figure 13: Some of the final state interaction diagrams which do not contribute to gluon production in pA collisions in $A_+ = 0$ light cone gauge.

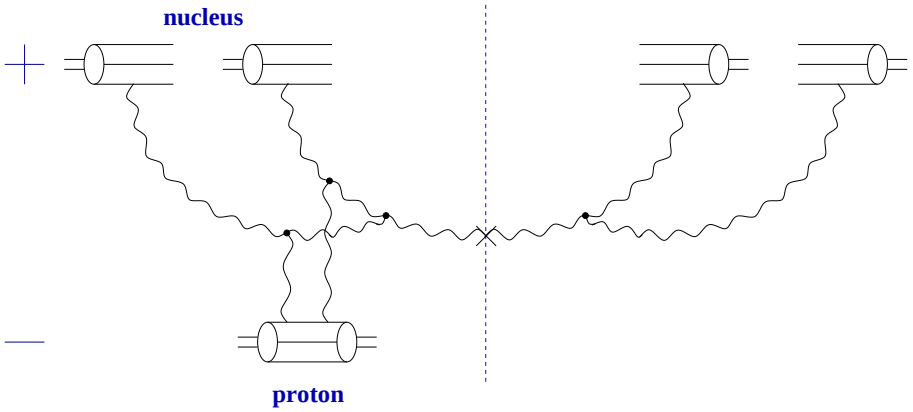

Figure 14: A virtual diagram which does not contribute to the gluon production process in pA collisions in $A_+ = 0$ light cone gauge. Triple gluon vertices are marked with black dots.

Now the generalization to the nucleus–nucleus (AA) case appears much more straightforward!

We conjecture that the following classes of diagrams with final state interactions cancel in AA:

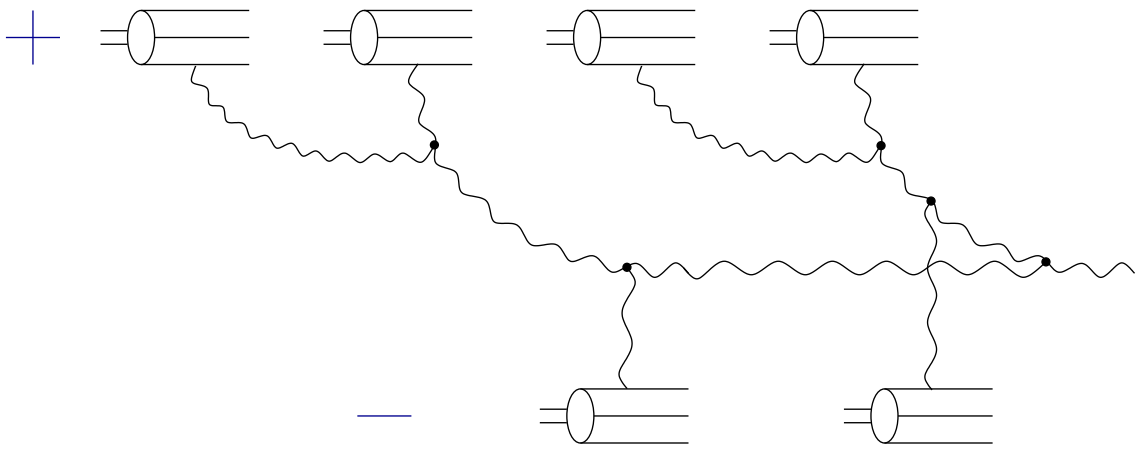

Figure 15: An example of a diagram which is not included in the gluon production mechanism in AA.

Nucleus–Nucleus Collisions (AA)

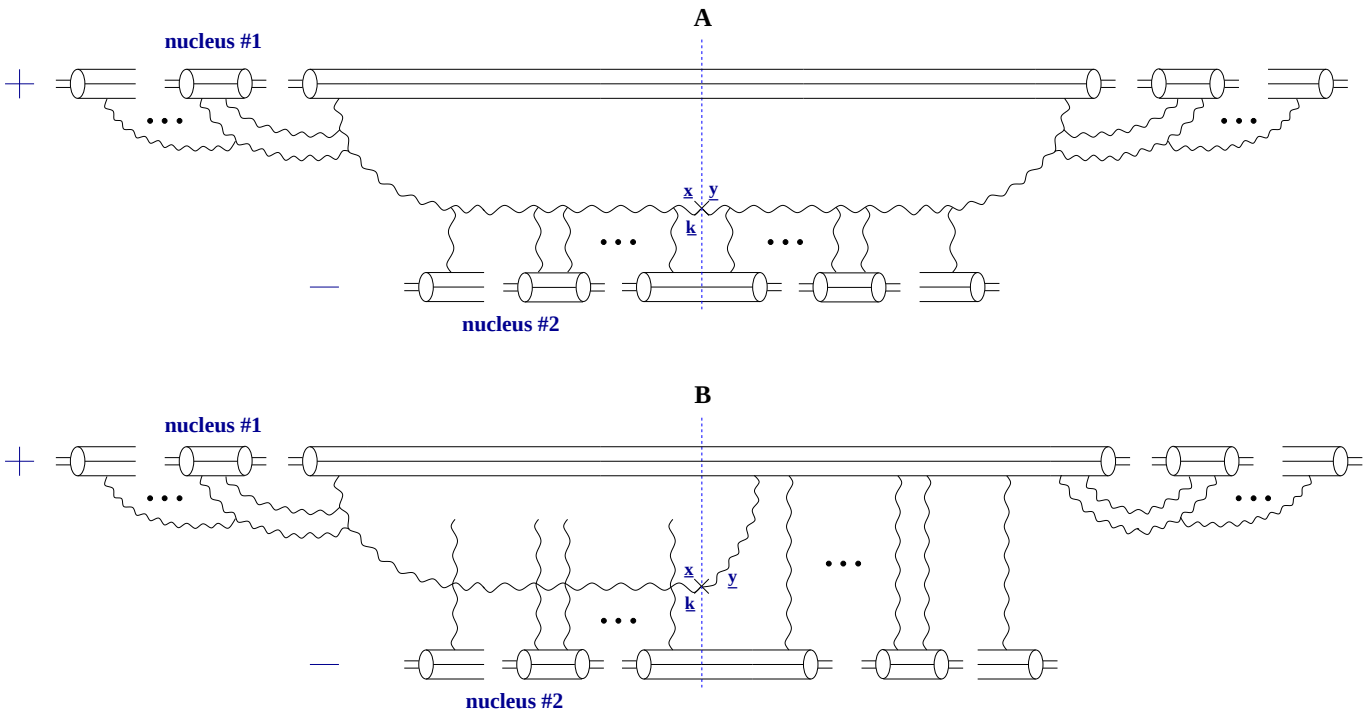

Figure 16: Diagrams contributing to the gluon production in nucleus-nucleus collisions in the $A_+ = 0$ light cone gauge.

$$\frac{dN^{AA}}{d^2k\,d^2b\,dy} = \frac{2\,C_F}{\alpha_S\pi^2}\left\{-\int\frac{d^2z}{(2\pi)^2}\,e^{i\underline{k}\cdot\underline{z}}\,\frac{1}{\underline{z}^2}\,\left(1-e^{-\underline{z}^2\,Q_{s1}^2/4}\right)\right.$$

$$\times\left(1-e^{-\underline{z}^2\,Q_{s2}^2/4}\right)+\int\frac{d^2x\;d^2y}{(2\pi)^3}\,e^{i\underline{k}\cdot(\underline{x}-\underline{y})}\,\frac{\underline{x}}{\underline{x}^2}\cdot\frac{\underline{y}}{\underline{y}^2}\,\left[\frac{1}{\underline{x}^2\,\ln\frac{1}{|\underline{x}|\,\mu}}\right.$$

$$\times\left(1-e^{-\underline{x}^2\,Q_{s1}^2/4}\right)\,\left(1-e^{-\underline{x}^2\,Q_{s2}^2/4}\right)+\frac{1}{\underline{y}^2\,\ln\frac{1}{|\underline{y}|\,\mu}}\,\left(1-e^{-\underline{y}^2\,Q_{s1}^2/4}\right)$$

$$\left.\left.\times\left(1-e^{-\underline{y}^2\,Q_{s2}^2/4}\right)\right]\right\}.$$

Properties of the solution

In the logarithmic approximation the solution becomes:

$$\frac{dN^{AA}}{d^2k\,d^2b\,dy} = \frac{C_F}{\alpha_S 2\pi^3}\left[\frac{Q_{s1}^2}{\underline{k}^2}\left(e^{-\frac{\underline{k}^2}{Q_{s1}^2+Q_{s2}^2}} - e^{-\frac{\underline{k}^2}{Q_{s1}^2}}\right) + \right.$$

$$\left. + \frac{Q_{s2}^2}{\underline{k}^2}\left(e^{-\frac{\underline{k}^2}{Q_{s1}^2+Q_{s2}^2}} - e^{-\frac{\underline{k}^2}{Q_{s2}^2}}\right)\right].$$

This distribution is depicted below:

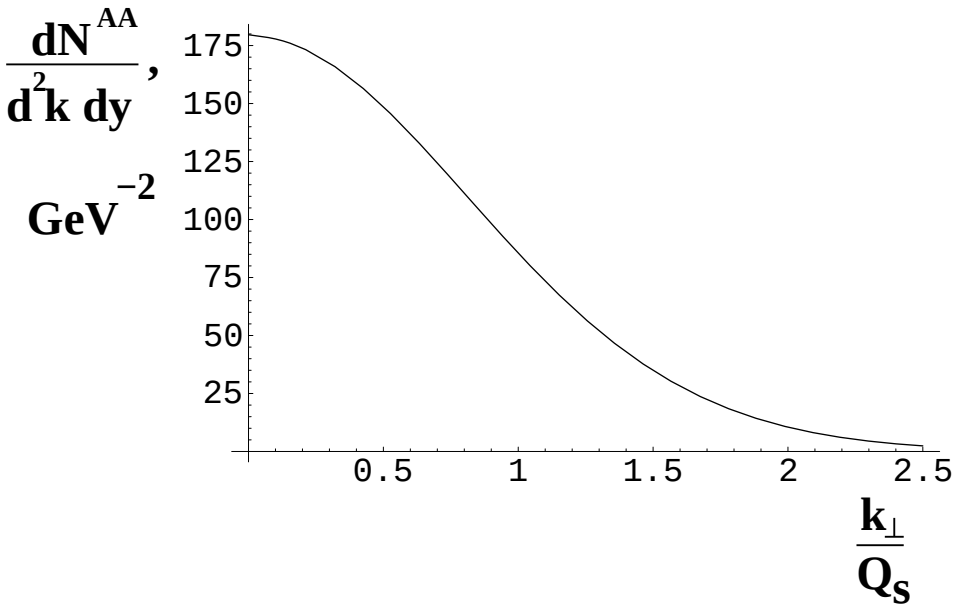

Figure 17: Distribution of the produced gluons for a central AA collision as a function of k/Q_s with the transverse area of the nuclei being $S_\perp = 50\,\mathrm{fm}^2$.

Note that the distribution is infrared safe:

$$\frac{dN^{AA}}{d^2k\,d^2b\,dy} \to \frac{C_F}{\alpha_S 2\pi^3} \quad \text{as} \quad \frac{k_\perp}{Q_s} \ll 1.$$

This means that the exact distribution can only have logarithmic $(\ln Q_s/k_\perp)$ divergence in the infrared !

$\Rightarrow$Multiple rescatterings do resolve the problem of the infrared divergence of the naive perturbative distribution !

In the ultraviolet limit the exact distribution reduces to the lowest order perturbative expression:

$$\frac{dN^{AA}}{d^2k\,d^2b\,dy} \sim \frac{Q_{s1}^2\,Q_{s2}^2}{\alpha_S\,\underline{k}^4} \quad \text{as} \quad \frac{k_\perp}{Q_s} \to \infty$$

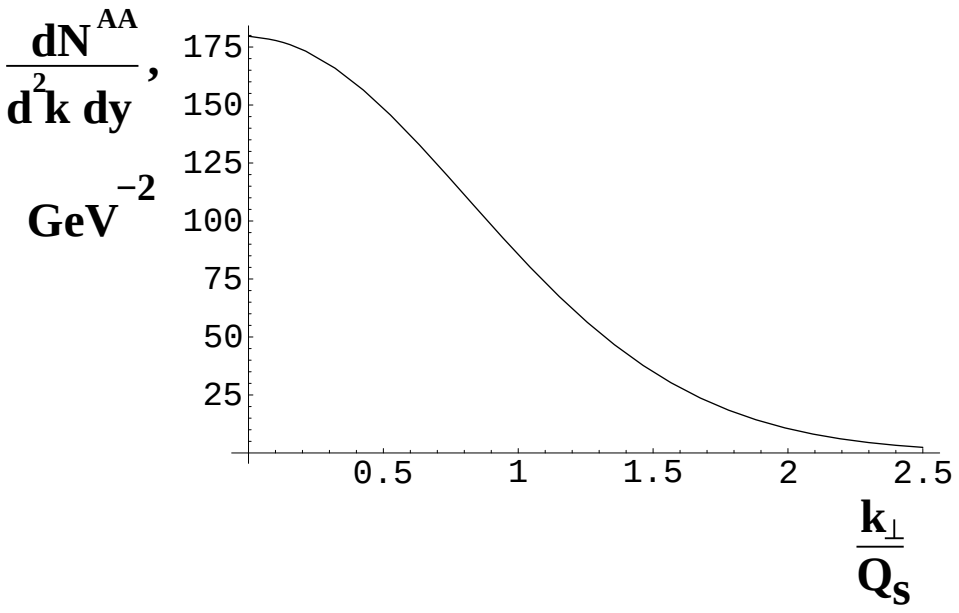

Figure 18: Distribution of the produced gluons for a central AA collision as a function of k/Q_s with the transverse area of the nuclei being $S_\perp = 50\,\mathrm{fm}^2$.

The average E_t per produced gluon given by this distribution for two identical nuclei is

$$< E_t >= \frac{\sqrt{\pi}(\sqrt{2}-1)}{\ln 2} Q_s \approx 1.06\, Q_s$$

$\Longrightarrow$The typical E_t and $k_\perp$ carried by a produced gluon are of the order of Q_s.

cf. A.H. Mueller, '99

What happens to the gluons in the collision?

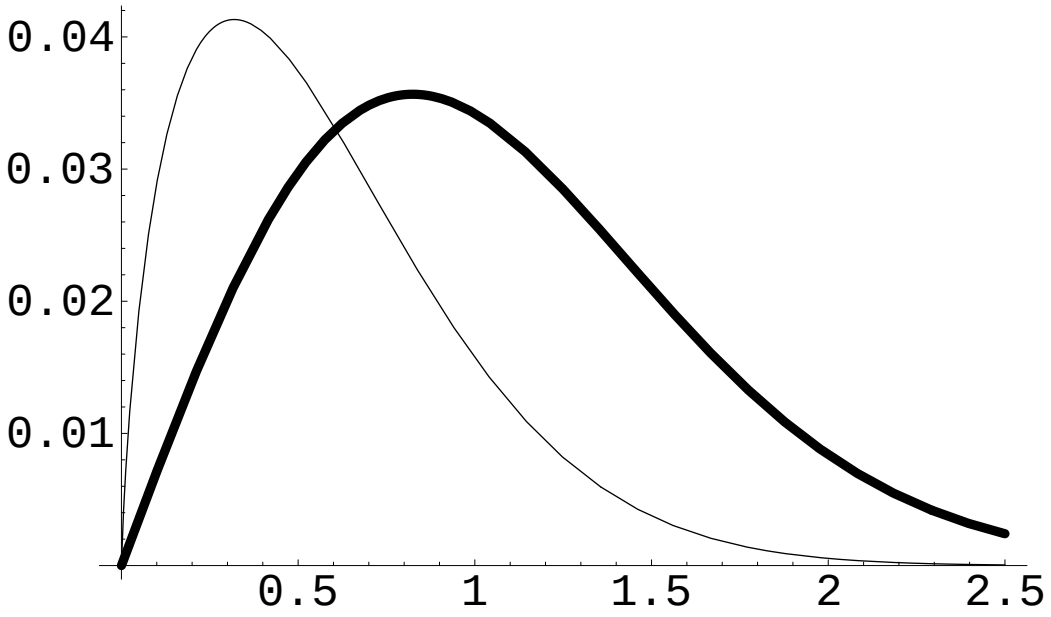

Figure 19: The gluon distribution multiplied by $k_\perp$ as a function of $k_\perp/Q_s$ in the one of the nuclei before the collision (thin line) and the gluon distribution after the collision (thick line).

The total number of gluons produced in the collision is

$$\frac{dN^{AA}}{d^2b\,dy} = \frac{C_F\,Q_s^2\,\ln 2}{\alpha_S\pi^2}.$$

Note: it's finite and cutoff independent!

It is proportional to the total number of gluons in one of the nuclei before the collision

$$\frac{dN^{AA}}{d^2b\,dy} \;=\; c\,\frac{dN^{WW}}{d^2b\,dy}.$$

Using the fact that the number of gluon in the nucleus before the collision is

$$\frac{dN^{WW}}{d^2b\,dy} \;=\; \frac{C_F\,Q_s^2}{\alpha_S\,2\,\pi^2}.$$

we conclude that the proportionality coefficient is

$$c \;=\; 2\,\ln 2 \;\approx\; 1.39$$

$\Rightarrow$ it is very close to the result of the numerical estimates of Krasnitz and Venugopalan giving $c = 1.29 \pm 0.09$

$\Rightarrow$ Agrees with phenimenological result of Kharzeev and Nardi with $c = 1.23 \pm 0.20$

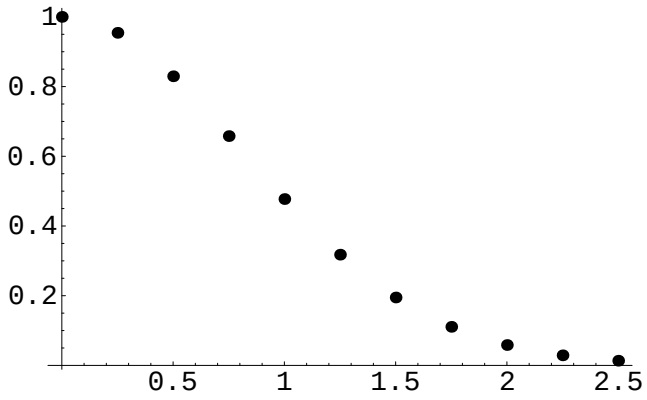

Figure 20: The gluon distribution found before represented as a set of dots schematically mimicking experimental data on distribution of produced particles.

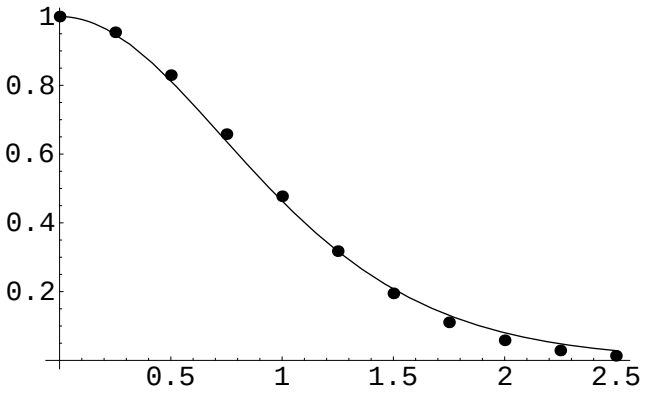

Figure 21: The same particle distribution fitted with relativistic Bose-Einstein thermal distribution function with $T = 0.4\,Q_s$ and $m = 1.5\,Q_s$.

Plus: The system with distribution close to thermal will easily thermalize into QGP.

Minus: Closeness of the two distributions makes them hard to distinguish experimentally!

Let us use recent PHOBOS data on multiplicity to estimate Q_s^2 at RHIC. PHOBOS (PRL 85, 3100 (2000)) reports the following total charged multiplicity per unit pseudorapidity in Au+Au collisions

$$\frac{dN_{ch}^{Au+Au}}{d\eta} = 555 \pm 12(\text{stat}) \pm 35(\text{syst})$$

at the center of mass energy $\sqrt{s} = 130\,\text{AGeV}$. Our result for a cylindrical nucleus is

$$\frac{dN^{AA}}{dy} = \frac{C_F\, Q_s^2\, S_\perp\, \ln 2}{\alpha_S \pi^2}.$$

Multiplying the PHOBOS result by $3/2$, and using a cylindrical nucleus approximation with $S_\perp = 50\,\text{fm}^2$ and $\alpha_s \approx 0.3$ we obtain

$$Q_s^2 \approx 2.1\,\text{GeV}^2 \quad \text{for } Au+Au \text{ at } \sqrt{s} = 130\,\text{AGeV}$$

which agrees with a much more carefull analysis of Kharzeev and Nardi (hep-ph/0012025) and is marginally inside of the small coupling region.

CONCLUSIONS

$\Rightarrow$ We have constructed the classical distribution of gluons in the state immediately following a heavy ion collision.

$\Rightarrow$ The typical transverse momentum $k_\perp$ and transverse energy E_t per produced gluon is of the order of saturation scale Q_s.

$\Rightarrow$ The distribution is IR finite up to logarithms, which is a clear advantage over the usual perturbative distribution.

$\Rightarrow$ The total number of the produced gluons is proportional to the total number of gluons inside the nuclear wave function before the collision with the proportionality coefficient $c = 2 \ln 2$.